

## APPLICATION OF MICROSCOPIC TECHNIQUES TO PIGMENT MANUFACTURE AND PERFORMANCE IN FLUID INKS†

THEODORE G. VERNARDAKIS

Sun Chemical Corporation, Pigments Division, Research and Operations Center, 4625 Este Avenue,  
Cincinnati, Ohio 45232, USA

### SUMMARY

*A number of physicochemical techniques including transmission electron microscopy, optical microscopy, densitometry, X-ray diffraction and surface area determinations were used in the study of organic pigment yellows in correlation with their performance characteristics in fluid inks. The pigment chosen for this study was Diarylide Yellow, CI Pigment Yellow 14, which is widely used in nitrocellulose-polyamide alcohol flexographic inks. Transmission electron microscopy was employed to obtain the particle size and shape of several preparations of the pigment (particle size distributions and average particle diameters). Crystallite size and average particle diameters were determined by X-ray diffraction line broadening and surface area techniques, respectively. Optical microscopy and densitometry were utilized to study properties of the flexographic ink films such as transparency and strength. The results show the significant effect on particle size caused by process variables in pigment manufacture such as drying conditions and use of additives such as solvents and surfactants. Variations in particle size are in turn related to differences in strength and transparency exhibited by the corresponding ink films.*

### 1. INTRODUCTION

Particle size and size distribution are perhaps the most important factors influencing the applicational properties of organic pigments. The particle size

† Presented at the 54th Colloid and Surface Science Symposium, Lehigh University, Bethlehem, Pennsylvania, June 15-18, 1980

and distribution of a pigment have a considerable effect on its tinting strength, rheology, gloss, opacity, lightfastness, and even upon its ease of dispersion.<sup>1-4</sup> One of the most effective techniques in obtaining particle size and distributions of finely divided materials is transmission electron microscopy; this technique reveals the shape of individual particles. Average crystallite sizes may be determined by X-ray diffraction line broadening techniques. X-ray diffraction also gives a measure of the degree of crystallinity of the pigment particles. Furthermore, surface area measurements can be used to evaluate average particle diameters. All three techniques can be utilized in determining particle dimensions and particle size distributions in organic pigment powders.

This study focuses on the effects of additives, such as solvents and surfactants, and of process variables, such as drying conditions, on the particle size of Diarylide Yellow pigments during their manufacture and isolation. Particle size variations are subsequently correlated with their performance characteristics in fluid inks. Visual, optical microscopic and densitometric techniques were employed in the investigation of applicational properties such as transparency—opacity, dispersion (floculation) and strength exhibited by the corresponding ink films.

The various physicochemical methods mentioned above can be used quite effectively in optimizing pigment manufacture for ink applications. In this paper the case history of a Diarylide Yellow pigment from initial manufacture to final ink assessment is followed.

## 2. MATERIALS AND EQUIPMENT

The pigment under investigation is the Diarylide Yellow (AAOT), CI Pigment Yellow 14 (21095), commonly known as AAOT Yellow.<sup>5</sup> It is prepared by the coupling of 3,3'-dichlorobenzidine with aceto-acet-*ortho*-toluidide (AAOT) and is shown in Fig. 1. For the purposes of this study, the pigment was prepared in the presence of several additives, and under different process

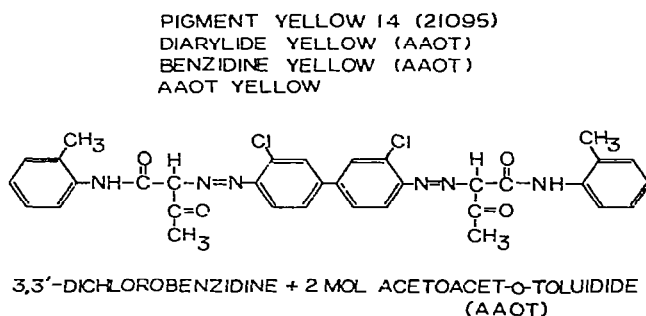


Fig. 1. AAOT Pigment Yellow 14, Diarylide Yellow AAOT, CI Pigment Yellow 14 (21095).

conditions in order to obtain particle size variability. The pigment was evaluated in nitrocellulose-polyamide alcohol flexographic inks, prepared by conventional ball milling techniques, and applied to the paper, foil, or polyethylene substrate with an anilox hand proofer.

The transparency–opacity of the ink films was determined visually. Strength was measured by densitometry using a Macbeth Densitometer, Model RD-219. This instrument measures diffuse reflection density (visual reflection density) which is in effect a measure of pigment strength exhibited by the ink films. Strength measurements were made from inks applied on coated stock. Optical microscopy was employed in the study of dispersion and flocculation. For this, a Zeiss Optical Microscope was used. Photomicrographs were obtained of liquid inks on covered slides and of ink films applied on plastic polyethylene film.

Particle size distributions of several pigment powders were obtained by Transmission Electron Microscopy (TEM). A JEOL JEM 200A Transmission Electron Microscope was used at magnifications of 30 000 $\times$  and 100 000 $\times$ . For the measurement, a minute amount of the sample was dispersed in absolute ethanol in an ultrasonic bath for a few minutes. A drop of the dispersion was placed on a graphite grid and allowed to dry. The grid was then inserted in the electron beam, for photomicrography. Particle size distributions were evaluated with a Carl Zeiss Particle Size Analyzer, Model TGZ3, 2269.

X-ray diffraction patterns were obtained with a General Electric XRD-5 X-Ray Diffractometer, using copper radiation with a nickel filter. The pigment powders were first slurried in an organic solvent. They were applied thickly on a glass slide, allowed to dry by evaporation, and then positioned on the diffractometer. Fast scans produced diffraction patterns from which the degree of crystallinity and probable variations in crystal structure of the samples could be determined. Slow scans of selected peaks were obtained from which crystallite size evaluations were carried out.

Specific surface area values by the BET method were obtained using a Quantasorb (Quantachrome Corporation) Surface Area Analyzer. This is a dynamic flow instrument which utilizes a constant flow of adsorbate gas through a small cell containing the sample. For the evaluation, the Quantasorb was used for single point determinations of BET surface areas with nitrogen used as the adsorbate gas, and adsorption carried out at the temperature of liquid nitrogen. Prior to adsorption the pigment samples were degassed by heating in a vacuum oven at 70°C overnight.

### 3. RESULTS OF TREATMENTS AND PROCESS VARIABLES

The results of the experimental treatments carried out on the various pigments are listed in Table 1, together with the corresponding opacity and strength of

TABLE 1  
EXPERIMENTAL TREATMENT OF THE VARIOUS SAMPLES OF AAOT PIGMENT YELLOW 14  
ALONG WITH THE OPACITY AND STRENGTH OF THE ALCOHOL FLEXOGRAPHIC INKS

Sample	Experimental treatment	Opacity <sup>a</sup>	Strength
1	No-surfactant—No solvent	1	0.94
2	No surfactant—Solvent A	2	0.99
3	No surfactant—Solvent B	5	1.04
4	Surfactant—No solvent	8	1.00
5	Surfactant—Solvent A	3	1.02
6	Surfactant—Solvent B	9	1.13
7	Surfactant—Solvent C	4	1.07
8	Surfactant—Solvent B—Air dried	7	1.12
9	Surfactant—Solvent B—Dried at 85°C for 3 days	6	1.03
10	Pigment as in No. 6—Refluxed in xylene for 1 h.	Transparent comp. to No. 7	0.69 (weak)

<sup>a</sup> Increasing numbers indicate a trend in increasing transparency

the subsequent alcohol flexographic inks. In the study the surfactant used was an amine type weakly cationic ethoxylated guanidine while the solvents used were Solvent A, hexadecane, the least polar; Solvent B, tetramethyl decynediol, the most polar and Solvent C, 2-ethylhexanol, of intermediate polarity.

The effect of the solvent on the transparency and strength of the ink films is quite evident from Table 1. In going from Sample 1 (no surfactant—no solvent) to Sample 2 (no surfactant—Solvent A) to Sample 3 (no surfactant—Solvent B) increases are obvious in both transparency and strength. The addition of a surfactant alone without any solvent as in Sample 4, again shows increases in transparency and strength over Sample 1.

The next area of study involved the addition of solvents in the presence of the surfactant as shown by Samples 5, 6 and 7. Of interest is the fact that not only the presence but also the polarity of the solvent is important in upgrading coloristic properties. With Sample 6, in the presence of the most polar Solvent B, major improvements were observed in both transparency and strength. Therefore the results clearly show that presence of the surfactant and use of solvent treatments produce stronger and more transparent pigments. Furthermore, solvent polarity is of importance, regardless of the presence (Samples 5, 6 and 7) or absence (Samples 2 and 3) of the surfactant. The more polar the solvent, the stronger and more transparent the resulting pigments. A measure of the degree of the transparency—opacity differences exhibited by certain selected products is shown in Fig. 2. For this purpose, the inks were applied on aluminum foil. Sample 7 was selected as the standard for comparisons, since it lay in the mid-range of the opacity—transparency scale.

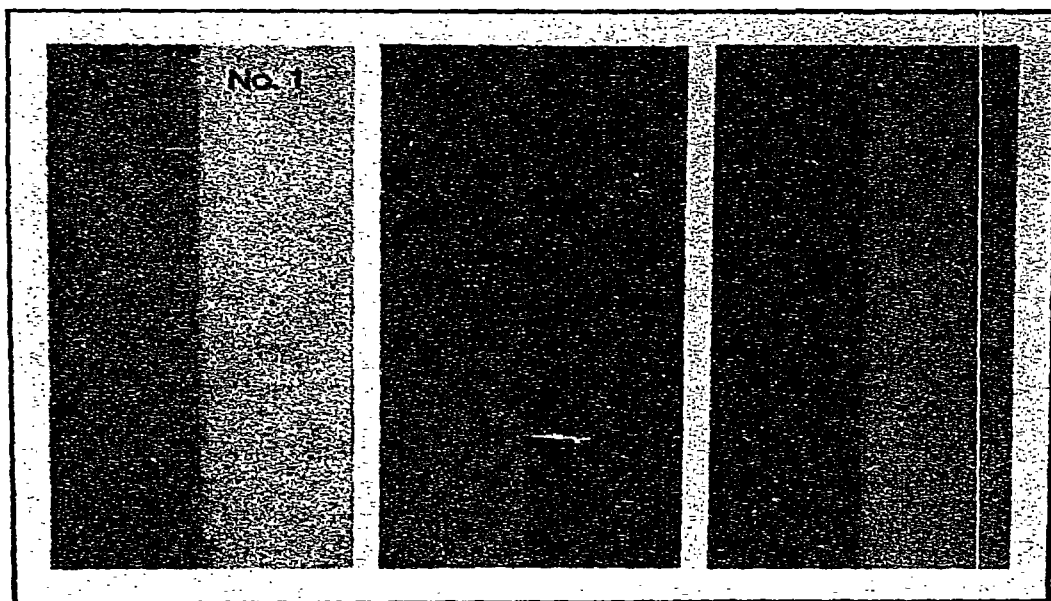


Fig. 2. Transparency–opacity differences between selected samples of AAOT Pigment Yellow 14.

The effect of drying conditions is also apparent from further review of Table 1. Standard drying of the pigment samples was taken at 85°C for 16 h. The colour properties of Sample 6 dried under these conditions were comparable to those of Sample 8, which was dried in ambient air. However, Sample 9 which was dried at 85°C for three days, became weaker and more opaque due to the much higher energy input during the drying process. This would be expected to result in the building up of the crystal or in the sintering of smaller particles to give a particle size above the optimum size of Sample 6. Therefore, prolonged drying is shown to have detrimental effects on the colour properties of this pigment type.

The building up of the pigment crystal can be deduced from a consideration of the data relating to Sample 10 in Table 1, formed by refluxing the dried powder from Sample 6 in xylene for 1 h. In this case, the pigment became transparent and quite weak when compared to Sample 7. From Table 1 it is evident that the strength of Sample 10 is considerably lower than that of Sample 7. The variation in transparency<sup>3</sup> is in accord with prior investigations found in the literature. At small particle sizes, pigments are transparent (Sample 6). As the particle size increases up to 0.1–0.2  $\mu\text{m}$ , pigments become opaque (Sample 1). Beyond that size, pigments become transparent<sup>3</sup> again (Sample 10) with improved lightfastness<sup>2</sup> but with considerable loss in strength.

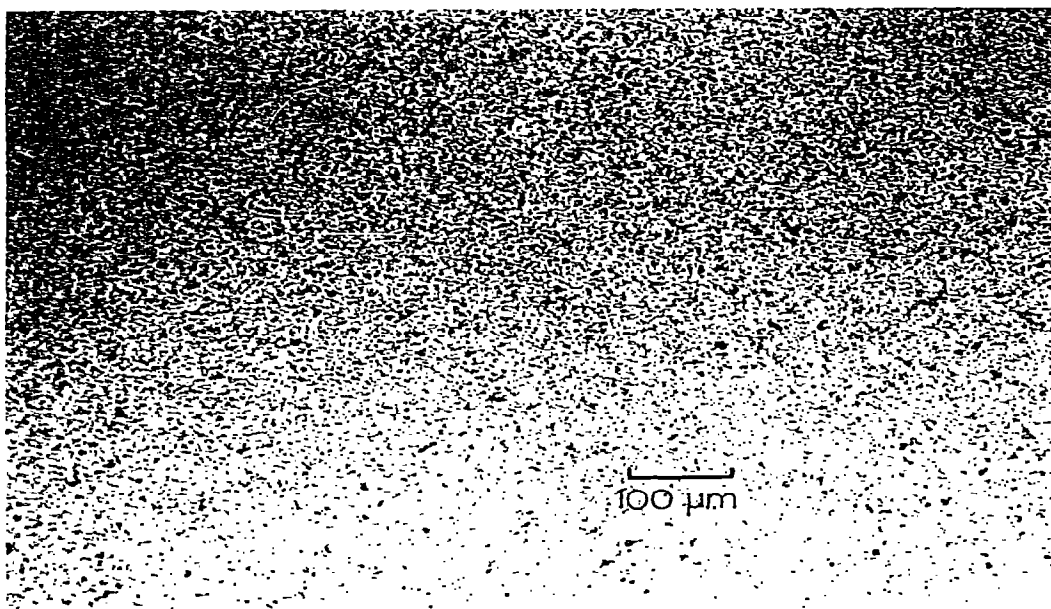


Fig. 3. Optical micrograph of liquid ink prepared with AAOT Pigment Yellow 14, Sample 1 showing flocculation (165 $\times$  magnification).

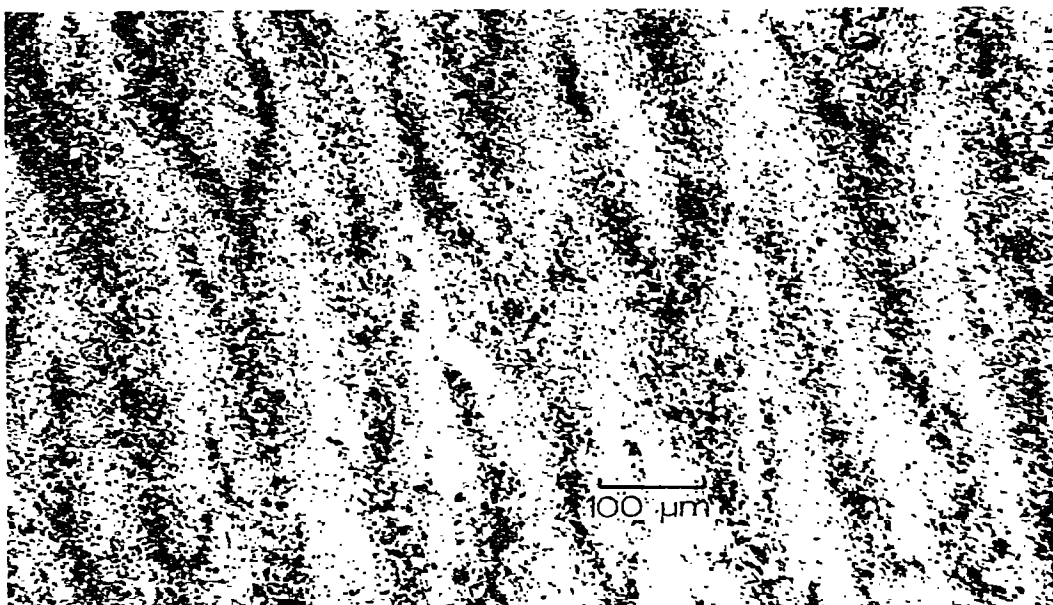


Fig. 4. Optical micrograph of dried ink film prepared with AAOT Pigment Yellow 14, Sample 1 showing flocculation (165 $\times$  magnification).

These effects become evident when the transmission electron micrographs are examined.

### 3.1. *Evidence of flocculation*

In order to show pigment flocculation in the flexographic inks, optical photomicrographs were obtained at magnifications of  $165\times$ . Figures 3 and 4 represent micrographs of the liquid ink on a glass slide with cover, and of the dried ink film on plastic polyethylene substrate, respectively, of Sample 1, and exhibit flocculation. Figures 5 and 6, on the other hand, represent micrographs of the liquid ink and dried ink, respectively, prepared with Sample 6, indicating that this is a non-flocculating pigment.

### 3.2. *Particle size distributions by transmission electron microscopy*

It has already been stated that the colour properties of the pigment samples under consideration are strongly affected by their particle size and distribution. Five of the pigments listed in Table 1 were selected for further study, as exemplifying best the variation in particle dimensions based on the differences in pigment treatment during the manufacture of AAOT Pigment Yellow 14.

Transmission electron photomicrographs were obtained for Samples 1, 2, 6, 7 and 10. These are represented in Figs 7-11. Visual inspection of the

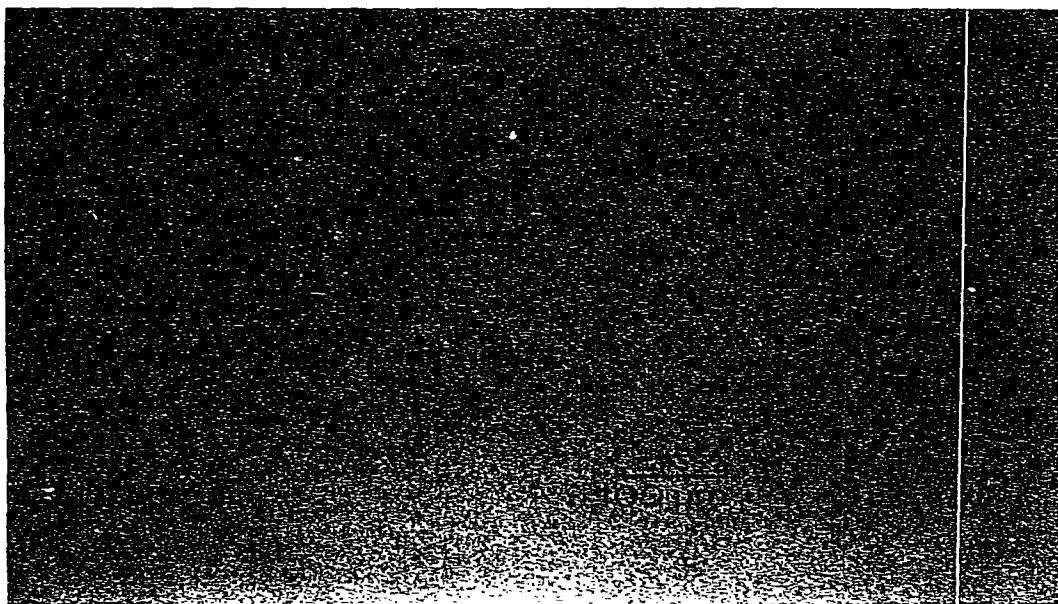


Fig. 5. Optical micrograph of liquid ink prepared with AAOT Pigment Yellow 14, Sample 6, non-flocculating ( $165\times$  magnification).

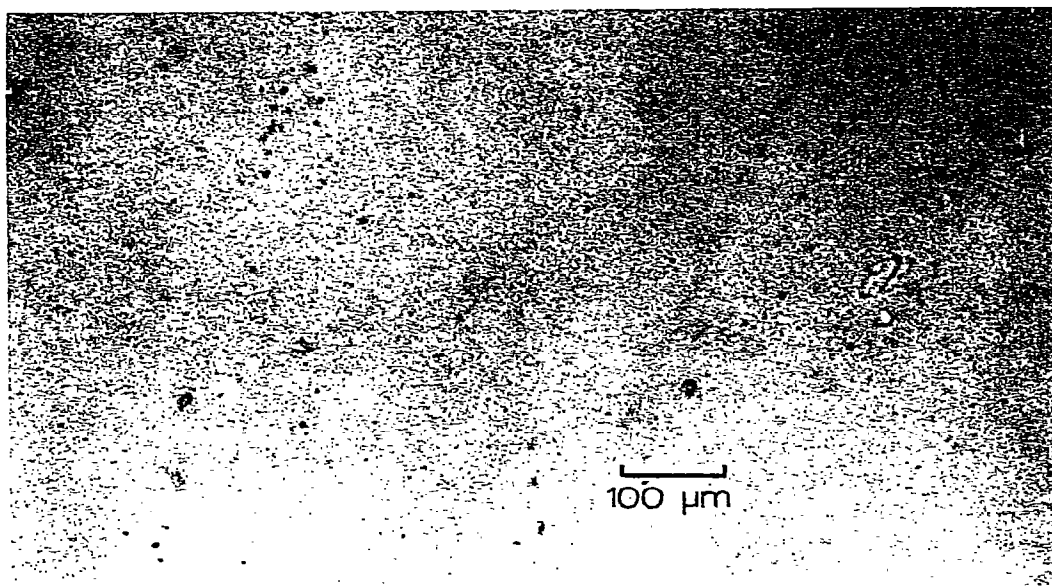


Fig. 6. Optical micrograph of dried ink film prepared with AAOT Pigment Yellow 14, Sample 6, non-flocculating (165 $\times$  magnification).

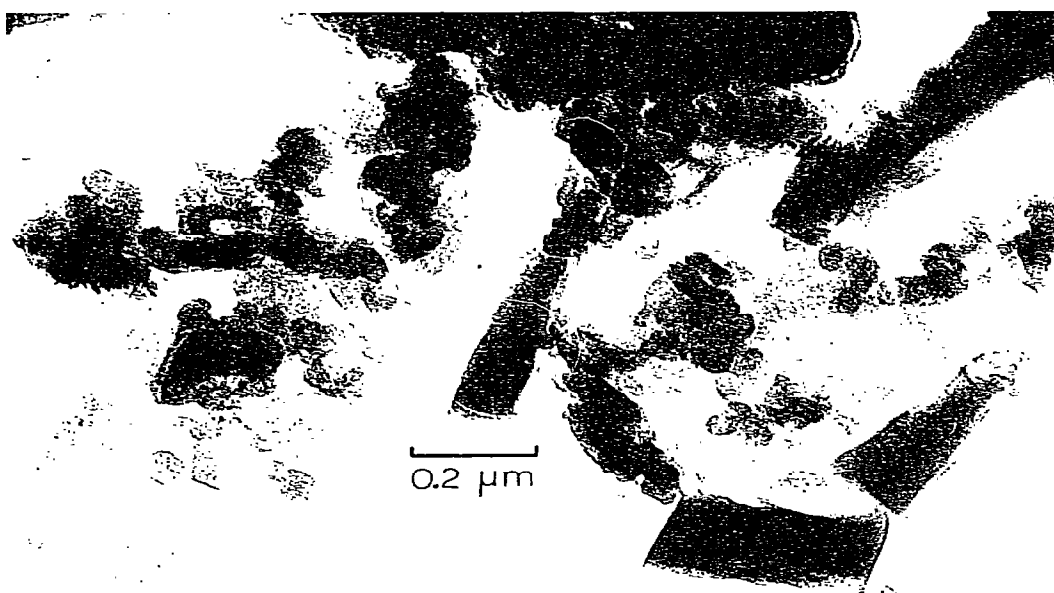


Fig. 7. Transmission electron-photomicrograph of AAOT Pigment Yellow 14, Sample 1 (100,000 $\times$  magnification).



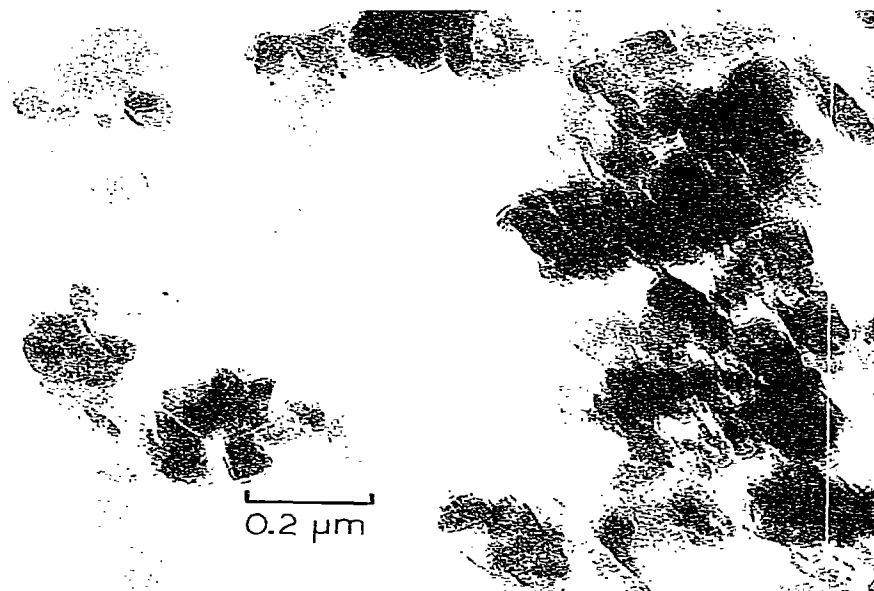


Fig. 8. Transmission electron photomicrograph of AAOT Pigment Yellow 14, Sample 2 (100 000 $\times$  magnification).

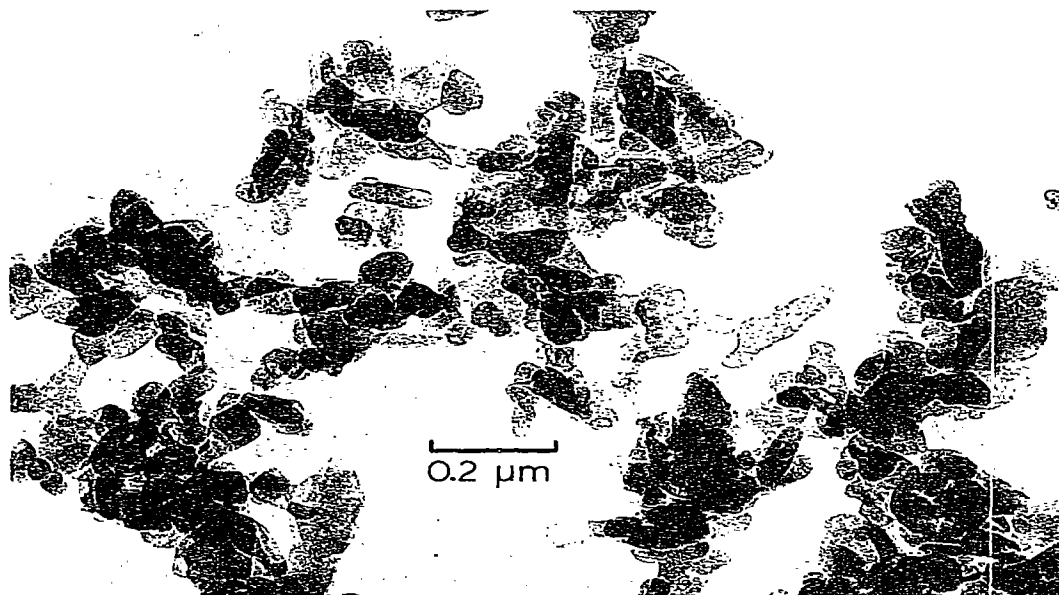


Fig. 9. Transmission electron photomicrograph of AAOT Pigment Yellow 14, Sample 6 (100 000 $\times$  magnification).

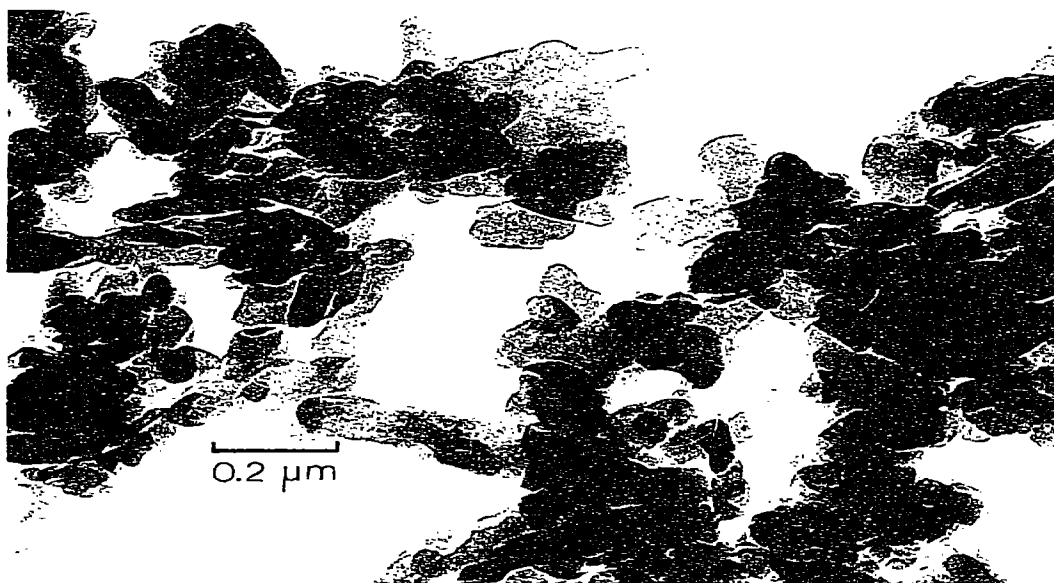


Fig. 10. Transmission electron photomicrograph of AAOT Pigment Yellow 14, Sample 7 (100,000 $\times$  magnification).

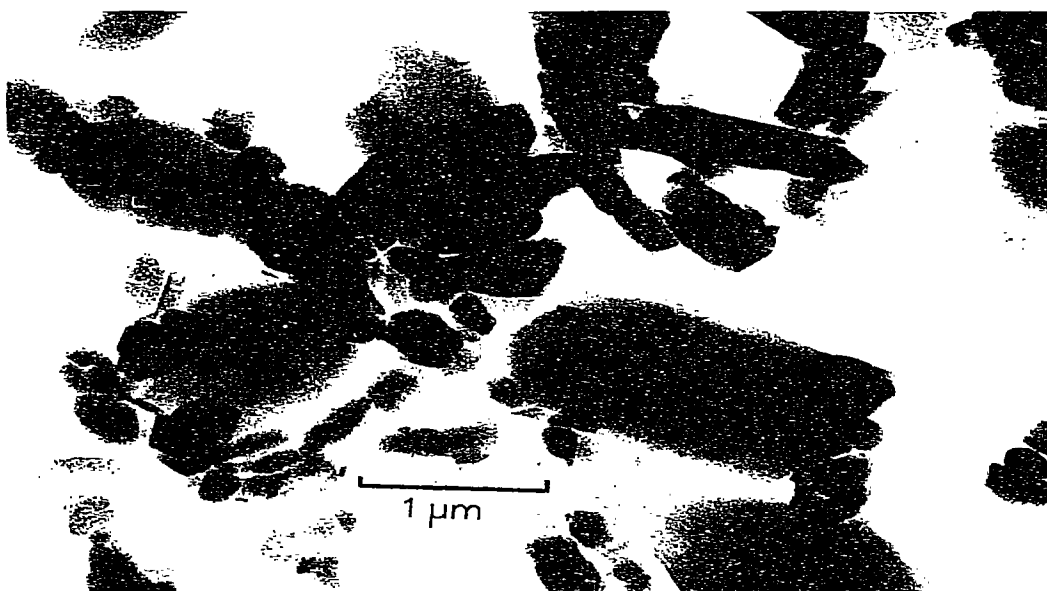


Fig. 11. Transmission electron photomicrograph of AAOT Pigment Yellow 14, Sample 10 (30,000 $\times$  magnification).

micrographs shows a decrease in size in going from Sample 1 to Sample 2 to Sample 6. In Sample 7, the dimensions increase above those of Sample 6. Sample 10 shows a considerable increase in particle size, over all previous samples. (It should be noted that Sample 10 was taken at a magnification of  $30\,000\times$  while the other samples were taken at  $100\,000\times$ .) The photomicrograph of Sample 10 shows excellent crystal formation with a high degree of crystallinity when viewed in conjunction with the X-ray diffraction data. A ( $30\,000\times$ ) photomicrograph of Sample 1, shown in Fig. 12, was taken in order to compare with the size of Sample 10 at the same magnification. The size variation between the two samples is quite evident from Figs 11 and 12. Figure 12 also shows large flocculates. This is in accord with micrographs of Figs 3 and 4, showing pigment flocculation in the inks. The photomicrograph of Fig. 9 for Sample 6 indicates a more uniform size and shape of the particles, in comparison with the other samples. It also exhibits a much more open particle network which would make this pigment not as highly flocculating as Sample 1.

The electron photomicrographs give a measure of particle shape as well. The shape ranges from equant to (mostly) columnar for all samples. In order to

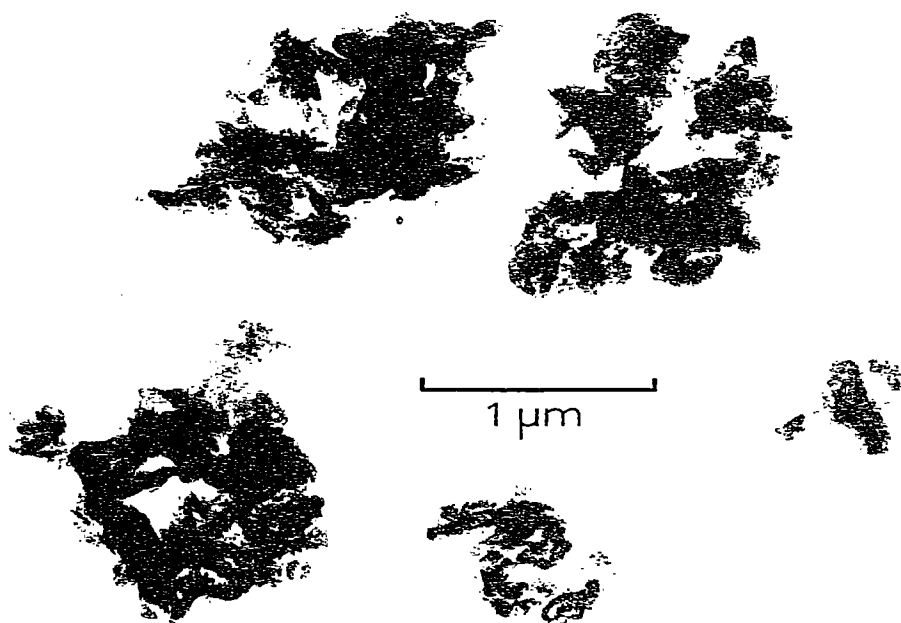


Fig. 12. Transmission electron photomicrograph of AAOT Pigment Yellow 14, Sample 1 ( $30\,000\times$  magnification).

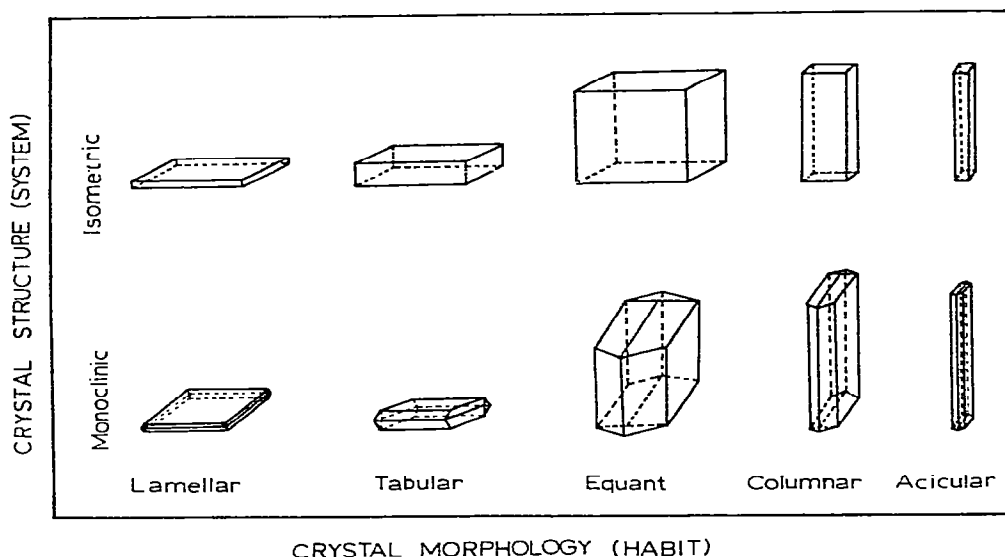


Fig. 13. Relation between crystal structure and crystal morphology.

facilitate the observations on particle shape Fig. 13 is included, showing variations in crystal morphology (habit) for isometric and monoclinic crystal structures (systems).

Determinations of particle size distributions were carried out for the five pigment samples from the photomicrographs utilizing a Carl Zeiss Particle Size Analyzer, Model TGZ3, 2269. The instrument focuses a beam of light on each particle on the micrograph which is adjusted to encompass the exact length of the particle under consideration. During the counting process each particle, depending on its size (length in this case), is registered in one of 48 compartments of varying dimensions. These dimensions depend on the magnification of the photomicrograph. For a magnification of 30 000 $\times$  the sizes that can be measured range between 0.0497 and 0.9143  $\mu\text{m}$ , while for 100 000 $\times$  they range between 0.0149 and 0.2743  $\mu\text{m}$ . When counting is completed, the number of particles having the same size is displayed in the appropriate compartment. By multiplying each number with the size of the corresponding compartment, the total diameter is obtained which when divided by the total number of particles, gives the value of the average diameter.

The particle size distributions are presented in graphical form by plotting the number of particles versus the size of each compartment which is, in effect, the diameter of those particles. Distribution curves having a jagged appearance are thus obtained. These curves are smoothed out and presented in Fig. 14 for the five samples of AAOT Pigment Yellow 14. Because of the much larger size of

Sample 10, a different scale for particle diameter was used in the figure. In addition, average particle diameter values were calculated for each sample. Pigment Sample 1 has a fairly flat distribution, ranging between 0.037 and 0.400  $\mu\text{m}$ . Average particle diameter is 0.104  $\mu\text{m}$ . The size distribution of Sample 2 is still relatively flat. The maximum of the curve, however, has moved to lower particle dimensions. The size ranges between 0.031 and 0.175  $\mu\text{m}$  with an average particle diameter at 0.086  $\mu\text{m}$ . Sample 6 exhibits a well-defined narrow bell-shaped distribution, with sizes ranging from 0.026 to 0.164  $\mu\text{m}$ . The average particle diameter has been reduced to 0.073  $\mu\text{m}$ . Sizes for Sample 7 are in the range of 0.031 to 0.186  $\mu\text{m}$ , with an average at 0.087  $\mu\text{m}$ . Again, the shape of the distribution curve is still quite narrow. When proceeding to Sample 10, the size distribution curve becomes fairly flat, with dimensions ranging between 0.031 and 2.07  $\mu\text{m}$ . The average size is quite large, at 0.421  $\mu\text{m}$ .

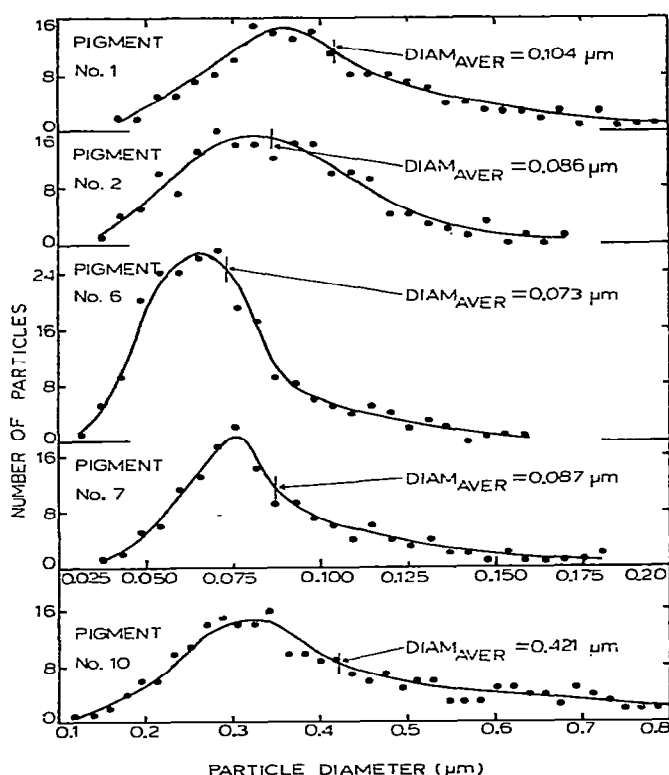


Fig. 14. Particle size distribution and average particle diameters of samples of AAOT Pigment Yellow 14.

TABLE 2  
RESULTS OF TRANSMISSION ELECTRON MICROSCOPY OF AAOT PIGMENT YELLOW 14

<i>Sample</i>	<i>Particle size distribution (<math>\mu\text{m}</math>)</i>	<i>Average particle diameter (<math>\mu\text{m}</math>)</i>	<i>Particle shape</i>
1	0.037–0.400	0.104	Few equant, most columnar
2	0.031–0.175	0.086	Few equant, most columnar
6	0.026–0.164	0.073	Columnar
7	0.031–0.186	0.087	Columnar
10	0.031–2.07	0.421	Few equant, most columnar

The results of transmission electron microscopy, in terms of particle size distribution, average particle diameter, and particle shape are listed in Table 2. The calculated values are in accord with the visual comparisons made from the photomicrographs. Furthermore, comparisons between the particle size distributions and the strength of the pigments in the liquid inks indicate that the smaller the size or the more narrow the distribution, the stronger the pigment should be. This is indeed the case, with Sample 6, the strongest and most transparent, from the consideration of Table 1. From Fig. 14 and Table 2, the narrow distribution and smallest average size for this pigment lead to the same conclusions of high strength and transparency. The narrowness of the distribution of Sample 7 would make this the second strongest pigment, and so on. The average size of Sample 7 is very close to that of Sample 2. Based on this fact alone, it would appear that Sample 2 should be of equal strength with Sample 7. This is not the case however, as the much narrower distribution curve exhibited by Sample 7 imparts higher strength in fluid ink application.

Sample 10 possesses the characteristic properties of a more lightfast diarylide pigment when compared to Samples 1, 2, 6 and 7 as exemplified by the results of Hafner.<sup>2</sup> This is apparent from the fact that it has a large average particle size and the highest degree of crystallinity when considered against the other four samples. From consideration of particle size alone, this should be a weak and transparent pigment. This is clearly the case, upon review of Table 1.

### 3.3. X-ray diffraction

X-ray powder diffraction patterns were obtained for Samples 1, 7 and 10, as shown in Fig. 15. The patterns are the same for all three, indicating that the crystal structure is the same. However, differences in the sharpness, intensity and resolution of the diffraction peaks would indicate that the degree of crystallinity is different among the three samples. Sample 10 should have the

highest crystalline character, with Samples 7 and 1 following, in that order. This result is in complete agreement with that derived from examination of the electron photomicrographs of Figs. 7, 10 and 11.

Since no crystal structure variation was observed for the various samples of AAOT Pigment Yellow 14, the X-ray diffraction pattern of this pigment is represented in Table 3. Tabulation is given in terms of  $2\theta$  angles in degrees and d-spacings in Ångstrom units, along with a relative measure of the intensity for each peak.

The X-ray results of Samples 1, 7 and 10 of the pigment are tabulated in Table 4. Pattern appearance, comments concerning crystallinity, and average crystallite size are included.

Crystallite size determinations were carried out on Pigments 1, 7 and 10 from an X-ray diffraction line broadening approach, using the Scherrer Equation according to Klug and Alexander,<sup>6</sup> and according to Rau's<sup>7,8</sup> work on oxide powders. Slow X-ray scans were obtained for the strongest peaks which show no interference. The experimentally observed half-peak width was then determined for each peak at the corresponding  $2\theta$  angles and the Scherrer

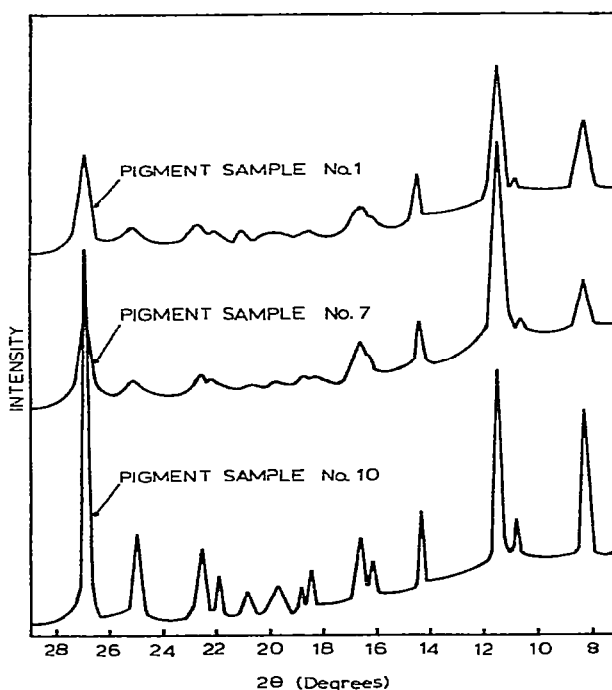


Fig. 15. X-ray diffraction patterns of samples of AAOT Pigment Yellow 14.

TABLE 3  
2 $\theta$  ANGLES AND  $d$ -SPACINGS OF AAOT PIGMENT YELLOW 14 FROM  
X-RAY DIFFRACTION PATTERNS

2 $\theta$ (degrees)	$d$ (Å)	$I^a$	2 $\theta$ (degrees)	$d$ (Å)	$I^a$
8.30	10.65	M	18.90	4.70	VW
10.80	8.19	VW	19.80	4.48	VW
11.50	7.69	MS	20.90	4.25	VW
14.35	6.19	W	21.95	4.05	VW
16.25	5.45	VW	22.60	3.93	W
16.65	5.32	W	25.00	3.56	MW
18.55	4.78	VW	26.87	3.32	S

<sup>a</sup> Intensity: S = strong, MS = medium-strong, M = medium, MW = medium-weak, W = weak, VW = very weak

Equation applied to evaluate crystallite sizes in the form below:

$$D = \frac{K\lambda}{\beta \cos \theta} \quad (1)$$

In eqn (1),  $D$  is the average crystallite size in Ångströms,  $K$  is the crystallite shape constant and equal to 0.9,  $\lambda$  is the X-ray wavelength,  $\theta$  is the Bragg angle in degrees, and  $\beta$  is the pure X-ray diffraction line broadening at half-maximum peak intensity ( $\beta_{1/2}$ ). What is actually measured experimentally is a quantity  $B$  in degrees which is corrected for instrumental broadening and in the case of copper radiation ( $\lambda = 1.542$  Å) for  $K_{\alpha_1\alpha_2}$ -doublet broadening.

In the case of the pigment under consideration, values of the  $B$  quantity were determined from X-ray diffraction line broadening of the peaks at  $2\theta = 11.50^\circ$  and at  $2\theta = 26.87^\circ$ . After making instrumental and  $K_{\alpha}$ -doublet broadening corrections, the quantity  $\beta$  was obtained. Application of the Scherrer Equation

TABLE 4  
X-RAY RESULTS OF AAOT PIGMENT YELLOW 14

Sample	Pattern appearance	Comments	Average crystallite size ( $\mu\text{m}$ )
1	Broad and diffuse line pattern	Poor crystallinity or very small crystallite size	0.028 <sup>a</sup> and 0.020 <sup>b</sup>
7	Slightly sharper pattern than Pigment 1	Slightly higher crystallinity or smaller crystallite size than Pigment 1	0.023 <sup>a</sup> and 0.020 <sup>b</sup>
10	Very sharp pattern	High crystallinity or larger crystallite size than both Pigments 1 and 7	0.056 <sup>a</sup> and 0.067 <sup>b</sup>

<sup>a</sup> From the X-ray diffraction line broadening of the peak at  $2\theta = 11.50^\circ$

<sup>b</sup> From the X-ray diffraction line broadening of the peak at  $2\theta = 26.87^\circ$



resulted in the values of the average crystallite sizes, which are listed in the last column of Table 4. Although these values do not agree numerically with those obtained from TEM (Table 2), they still show the same trend, i.e., small crystallite size for Sample 7, larger for Sample 1 and largest for Sample 10.

Worthy of note is the fact that the values calculated from the two peaks at  $11.50^\circ$  and  $26.87^\circ$  are not the same. This indicates very clearly the shape differences of length, width and thickness that exist in a pigment crystal (Fig. 13). If the crystal structure of the pigment were known exactly, then one would be in a position to assign each of the numbers obtained to either the length, width or thickness of the crystal. This becomes evident when considering the results reported by Klug and Alexander<sup>6</sup> on the crystallite shape of nickel hydroxide (ref. 6, p. 513) and by Rau<sup>9</sup> on beryllium oxide.

### 3.4. Surface area

The specific surface area of Samples 1 and 7 were determined by using the Quantasorb Surface Area Analyzer. The single point BET method was employed.<sup>10</sup> The instrument was used for single point BET analysis in order to take advantage of the ease and speed of operation in routine surface area calculations. The experimental results are shown in Table 5. As expected, Sample 7, possessing a smaller particle size, has a higher specific surface area than Sample 1.

The BET surface area may be used to calculate the specific surface diameter of the particles.<sup>11</sup> This is done by using eqn (2) below in the form:

$$D = \frac{6}{\rho S} \quad (2)$$

where  $D$  is the average particle diameter in  $\mu\text{m}$ ,  $\rho$  is the pigment density, and  $S$  is the specific surface area in  $\text{m}^2 \text{g}^{-1}$ . The density of AAOT Pigment Yellow 14 was taken as  $1.43 \text{ g cm}^{-3}$ . The derivation of eqn (2) was based on the assumption that all particles are spherical in shape. From the TEM results, it is known that this is not true. Therefore, values of the average particle diameter from eqn (2) will not be in good agreement with those from the TEM method. However, size trends may be obtained.

The results of average particle diameter from surface area are listed in Table

TABLE 5  
SURFACE AREA AND AVERAGE PARTICLE DIAMETER OF AAOT  
PIGMENT YELLOW 14

Sample No.	Surface area ( $\text{m}^2/\text{g}$ )	Average particle diameter from surface area ( $\mu\text{m}$ )
1	25.3	0.166
7	28.8	0.146

5. As expected, Sample 7 has a smaller particle size than Sample 1. In comparison with the average size of the same samples from Table 2, these values are higher, due to the assumptions made in the derivation of eqn (2).

#### 4. CONCLUSIONS

In the course of this investigation, it has been shown that additive treatments and process variables have an important effect on the particle size and size distributions of diarylide pigment powders. Particle size distributions, in turn, affect strongly the coloristic properties of the pigment when used in fluid inks. Properties such as strength, transparency, and dispersion can be optimized during pigment manufacture by a variation in the additive treatments or in the process during preparation and isolation of the pigment. Considerable improvement in these properties has been obtained when the particle size distribution of the pigment is kept in a narrow range.

The physicochemical techniques employed have proven invaluable in the elucidation of the particulate structure of the pigment either in the ink form, or in the powder form. The results obtained from transmission electron microscopy, X-ray diffraction, and surface area measurements in terms of particle size distributions, average particle diameters, crystallinity and specific surface area have been related very effectively to the variations observed in strength, transparency, flocculation and lightfastness. These latter properties were determined from the fluid inks through the application of optical microscopy, densitometry and visual observations. These techniques can therefore be used routinely in optimizing pigment manufacture and pigment performance not only in fluid inks but in many other applications.

#### ACKNOWLEDGMENTS

The author wishes to acknowledge the assistance of Colin Campbell and Karen Root for the pigment and ink preparations, and of Jack Vass for the preparation of the photomicrographs. Acknowledgment is also due to Dr H. M. Smith, Research Director, and Dr G. H. Robertson, Research Manager, Pigments Division, Sun Chemical Corporation, for their encouragement and permission to publish this paper.

#### REFERENCES

1. F. M. SMITH, *J. Oil Col. Chem. Assoc.*, **58**, 205 (1975).
2. O. HAFNER, *J. Paint Technol.*, **47**, 9 (1975).
3. D. M. VARLEY and H. H. BOWER, *J. Oil Col. Chem. Assoc.*, **62**, 401 (1979).

4. T. SATO, *J. Coatings Technol.*, **51**, 79 (1979).
5. L. SHAPIRO, in *Pigment handbook*, Vol. 1, ed. T. C. Patton, p. 555. New York, John Wiley & Sons, Inc. (1973).
6. H. P. KLUG and L. E. ALEXANDER, *X-Ray diffraction procedures for polycrystalline and amorphous materials*, p. 491, New York, John Wiley & Sons, Inc. (1954).
7. R. C. RAU, in *Advances in X-ray analysis*, Vol. 5, ed. W. M. Mueller, p. 104, New York, Plenum Press, Inc. (1962).
8. R. C. RAU, in *Advances in X-ray analysis*, Vol. 6, eds. W. M. Mueller and M. Fay, p. 191. New York, Plenum Press, Inc. (1963).
9. R. C. RAU, *J. Amer. Ceram. Soc.*, **47**, 179 (1964).
10. S. LOWELL, *Introduction to powder surface area*, p. 34, New York, John Wiley & Sons, Inc. (1979).
11. C. ORR, Jr., in *Pigment handbook*, Vol III, ed. T. C. Patton, p. 127. New York, John Wiley & Sons, Inc. (1973).